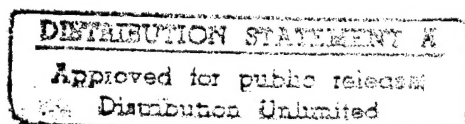NASA Contractor Report 194915

Characterization of Spacecraft and Environmental Disturbances on a SmallSat

Thomas A. Johnson, Dung Phu Chi Nguyen, and Vince Cuda
CTA Incorporated
Hampton, Virginia

Doug Freesland
CTA Defense Systems Incorporated
McLean, Virginia

19950710 009

CHARACTERIZATION OF SPACECRAFT AND ENVIRONMENTAL DISTURBANCES ON A SMALLSAT

Thomas A. Johnson

Dung Phu Chi Nguyen

Dr. Vince Cuda

CTA INCORPORATED
1 Enterprise Parkway Suite 390
Hampton, VA 23666
(804) 827-1847

Doug Freesland

CTA Defense Systems Incorporated
1521 Westbranch Drive
Mclean, VA 22102-3201
(703) 883-1000
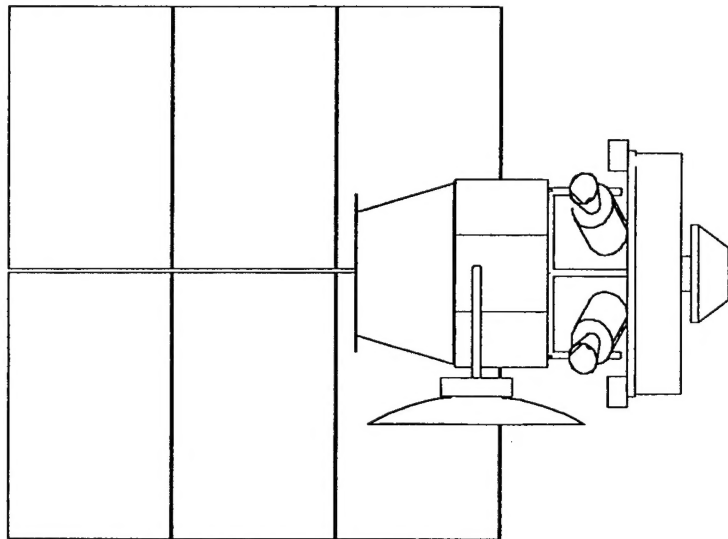
This page was intentionally left blank.

OUTLINE

- Introduction
- Mission Selection
- Simulation Techniques
- Disturbances
- Analysis Results
- Conclusions

This page was intentionally left blank.

INTRODUCTION

Introduction

Commercial development of small satellites (SmallSats) opens up the opportunity to fly more sophisticated payloads in less time and for less money than larger satellites. SmallSats are generally defined as spacecraft that are in the 150 to 500 kilogram weight class and can be launched to orbit with a Pegasus or Scout class launch vehicle. The present environment of limited fiscal resources forces the need for a more cost effective approach to remote sensing missions. SmallSats are being considered for Earth observing and microgravity experiments because they can be launched at a lower cost and developed in less time.

Introduction

- Commercial development of small satellites (SmallSats) opens up the opportunity to fly dedicated payloads

- SmallSats can be launched for lower costs and in less time than larger satellites

- SmallSats are being considered for remote sensing and microgravity experiments

- This study focused on SmallSats (150-500 kg) that could be accommodated by a Scout or Pegasus size launch vehicle

Objectives

The objective of this study is to model the on-orbit vibration environment encountered by a SmallSat. Vibration control issues are common to the Earth observing, imaging, and microgravity communities. A spacecraft may contain dozens of support systems and instruments, each a potential source of vibration. The quality of payload data depends on constraining vibration so that parasitic disturbances do not affect the payload's pointing or microgravity requirement.

In practice, payloads are designed incorporating existing flight hardware in many cases with nonspecific vibration performance. Thus, for the development of a payload, designers require development of a thorough knowledge of existing mechanical devices and their associated disturbance levels. This study will evaluate a SmallSat mission and will seek to answer basic questions concerning on-orbit vibration.

8

Objective

- This study seeks to characterize to on-orbit vibration environment encountered by SmallSat missions

- This study helps to answer some basic questions:

    - Can SmallSat buses provide the pointing precision and jitter control required by "EOS-like" payloads?

    - Do SmallSat on-board disturbances exceed payload jitter requirements?

    - Can SmallSats take advantage of control for the reduction of on-board jitter?

This page was intentionally left blank.

MISSION SELECTION

This page was intentionally left blank.

Mission Selection

- Payload and spacecraft identification

- Payload selection

- Spacecraft Bus selection and definition

- Orbit selection

Identification of Potential SmallSat User

Payloads were considered from the Earth observing, microgravity, and imaging communities. Candidate payload requirements were matched to spacecraft bus resources of present day SmallSats. From the set of candidate payloads listed in Appendices A and B, a representative payload was selected.

Identification of Potential SmallSat Users

- Payload were considered from the Earth observing, microgravity, and imaging communities

- Candidate payload requirements were matched to spacecraft bus resources of present day SmallSats

- Emphasis was placed upon payloads that could take advantage of a SmallSat flight opportunity

15

Earth Observing System (EOS)

Selection of a potential EOS payload began by separating the instruments into four weight classes and classifying the placement capability of the spacecraft buses into three categories. An increase in the placement pointing capability expands the number of candidate spacecraft buses. For example, 5 EOS instruments can take advantage of the 135 kg launch service, however, an increase in placement pointing of 36 arcsec (e.g., via the use of a CSI technology) could provide up to 14 instrument candidates. These instruments are listed and describe in Appendix A. The instrument data are extractions of instrument parameters given in the 1993 EOS Reference Handbook.

The following table summarizes the results of the placement capability study.

Weight Class (kg)	> 3600 arcsec	> 360 arcsec	>36 arcsec
45	4	6	6
70	5	8	8
115	5	11	12
135	5	12	14

The following table categorizes the jitter and stability requirements of the manifested EOS instruments into three groups.

(arcsec/sec)	Number of Payloads with pointing requirement
<10	2
<50	4
<100	7

After evaluating individual instruments and comparing the jitter requirements, the payload that required the tightest jitter control was selected to represent a typical EOS payload. The philosophy is that if the tightest jitter requirement was met then the remaining payloads could be supported on a SmallSat.

Earth Observing System (EOS)

- Thirty eight EOS payloads were considered

- EOS payloads are good candidates for SmallSat missions due to their modest resource needs

- Payload control requirements ranged from 5400 to 90 arcsecs

- Payload jitter requirements ranged from 360 to 2 arcsecs per second

- Spacecraft jitter appears to be the most significant concern for EOS payloads

Microgravity Sciences

To date, the majority of microgravity experiments have been performed on manned carriers or recoverable unmanned carriers. Not much interest has been expressed in non-recoverable microgravity experiments since the resultant sample from the experiment is in most cases the primary source of data. This is particularly true in the areas of materials science and biotechnology.

Non-recoverable microgravity experiments may be possible in the area of fundamental science, which includes the study of the behavior of fluids, transport phenomena, condensed matter physics, and combustion science. Experiments in fluids and combustion present opportunities because the experiment data is primarily video and environmental measurements, not a sample. A brief examination of existing microgravity experiments shows that there is no available experiment hardware that can be flown on a SmallSat (135 kg class.) It may be possible to adapt particular pieces of experiment hardware to fly on a non-recoverable SmallSat. These experiments would require the addition of certain capabilities such as video and data downlink. Also, certain processes of the experiment may require automation (e.g., the transfer of fluids from one container to another).

Of the non-recoverable candidates identified, the Interface Configuration Experiment (ICE), a small Spacelab glovebox fluids experiment; the Pool Boiling Experiment (PBE), operated in a Get Away Special (GAS) container in the orbiter cargo bay; and the Phase Partitioning Experiment (PPE), a small middeck fluids experiment, would require minimal resources and the addition of a video system/data downlink for observing the experiment results.

The recoverable experiments are primarily in the areas of biotechnology and materials science and require the return of a physical sample. In order to transform the recoverable experiments into non-recoverable experiments; the addition of capabilities may be required, such as the automation of certain processes of the experiment.

Of the recoverable candidates identified, the Protein Crystal Growth (PCG) experiment would require automation of the sample mixing process and a video capability to observe the crystals prior to recovery (a similar commercial experiment is planned for use on the COMET recovery module). The internal Space Acceleration Measurement System (SAMS) would require modification of its data system. Rather than storing data on optical disks that require changeout during the mission, the data would have to be downlinked.

Microgravity Sciences

- Microgravity levels are expected to be lower for SmallSats than for Shuttle missions

- Twenty four microgravity payloads were considered during this study

- The microgravity requirement is $10-6$ to $10-3$ g over the 0.01 to 300 Hz frequency range

- (Automated) Space Shuttle Glove Box experiments show the most promise for conversion to a non-recoverable SmallSat flight

- Crystal growth and combustion experiments are potential candidates for recoverable SmallSat missions

Imaging Payloads

Imaging payloads must also account for spacecraft jitter. Industry has made the call for on-orbit sensing that can provide multi-look, multi-spectral, high-resolution images of both the land and the oceans of this planet. The majority of images are provided by either SPOT or LandSat resources and resolutions are limited to the 10-30 meter range. As demand for more detailed mapping increases, industry is considering imaging that approaches the 1-3 meter range from orbits up to 700 Km. This translates into sub-arcsec pointing requirements that need to be met by on-board imaging instruments. The need for jitter control will be critical for these missions and methods for mitigating disturbances are under consideration by payload developers.

Payload designs were solicited by the investigators to evaluate jitter disturbances and instrument requirements. Due to the competitive nature of this evolving market, responses to our requests were marginal. For the purpose of this study, insufficient description of the imaging payloads has forced us to eliminate them as a candidate mission for the numerical analysis.

20

Imaging Payloads

- Conventional imaging satellites now being flown are large and costly to launch

- Currently, several aerospace companies are considering SmallSats for imaging payloads

- Sub-arcsec pointing is required for high resolution ground imaging (but fast shutter times may bypass the jitter problem)

- Due to the competitive nature of this market, flight mission scenarios were unavailable for this study

Selection of Payload

The requirements of GLAS were considered very stringent for the 150 - 500 kg class of payloads. Once the payload was selected, a generic SmallSat was designed in order to accommodate the payload requirements (weight, size, power, etc.). This study seeks to characterize the on-orbit vibration environment of a SmallSat designed for this type of mission and to determine whether a SmallSat can provide the precision pointing and jitter control required for earth observing payloads.

Selection of Payload

- Selected Geoscience Laser Altimeter System (GLAS) payload to represent a typical mission because of its stringent jitter requirement

- GLAS has the following pointing and jitter requirements:
  - 90 arcsec pointing control
  - 2 arcsec/sec jitter control

- Microgravity calculations for SmallSats are deferred to later studies

This page was intentionally left blank.

Selection of Spacecraft Bus

- Modeled an eight-sided DSI Bus because data was readily available and is typical of SmallSats

- Modified the DSI Bus to accommodate the GLAS payload and the Attitude Control System (ACS)

- Modified the UARS ACS to provide spacecraft control
- Sized the solar array to accommodate resource requirements of GLAS and spacecraft

- Added high gain antenna for additional study
 - GLAS requires <200 kbps
  - DSI BUS Telemetry

Orbit Selection

This table presents the orbital parameters selected for the analysis. The parameters are based upon GLAS payload requirements.

Parameter	Value
Altitude	705 km
Rho	64.21964 deg
Orbital Period	98.87778 min
Orbital Rate	0.060681 deg/sec
Inclination	98.20795 deg
Sun Synchronous Inclination	98.20795 deg
Precession	0.9856 deg/day
Eccentricity	0
Max Umbra	35.27719 min
Sun Fraction	0.643224

Orbit Selection

- Orbital parameters were driven by payload requirements

- Spacecraft orbit was defined to study environmental forces on the spacecraft

10 ft.

6.5 ft.

39 in.

27 in.

30 in.

31 in.

(Not to Scale)

28
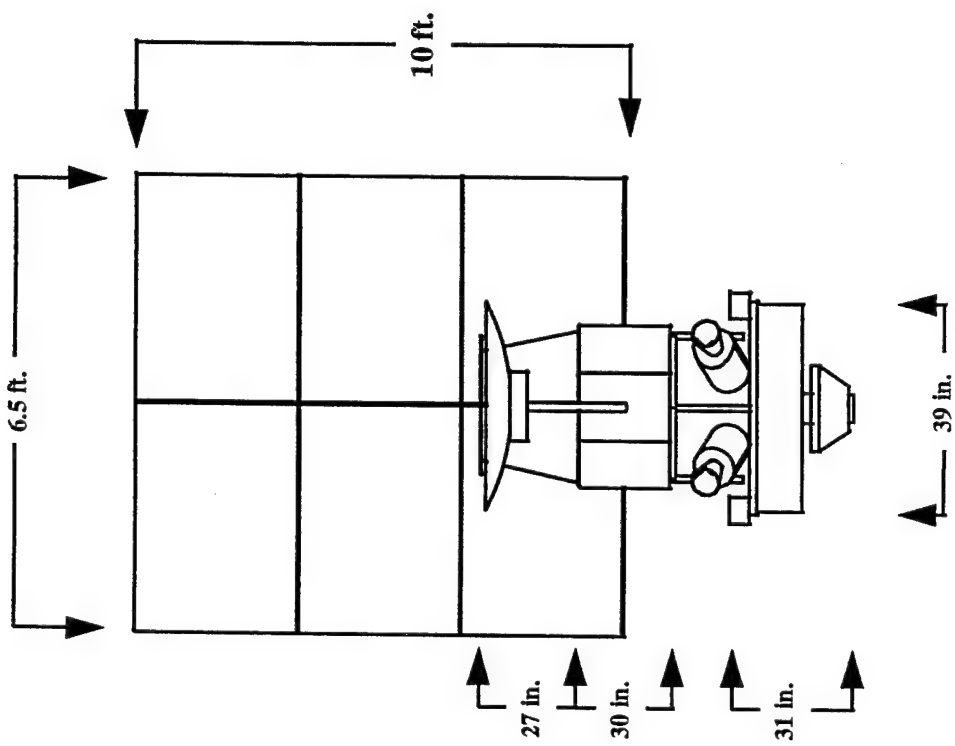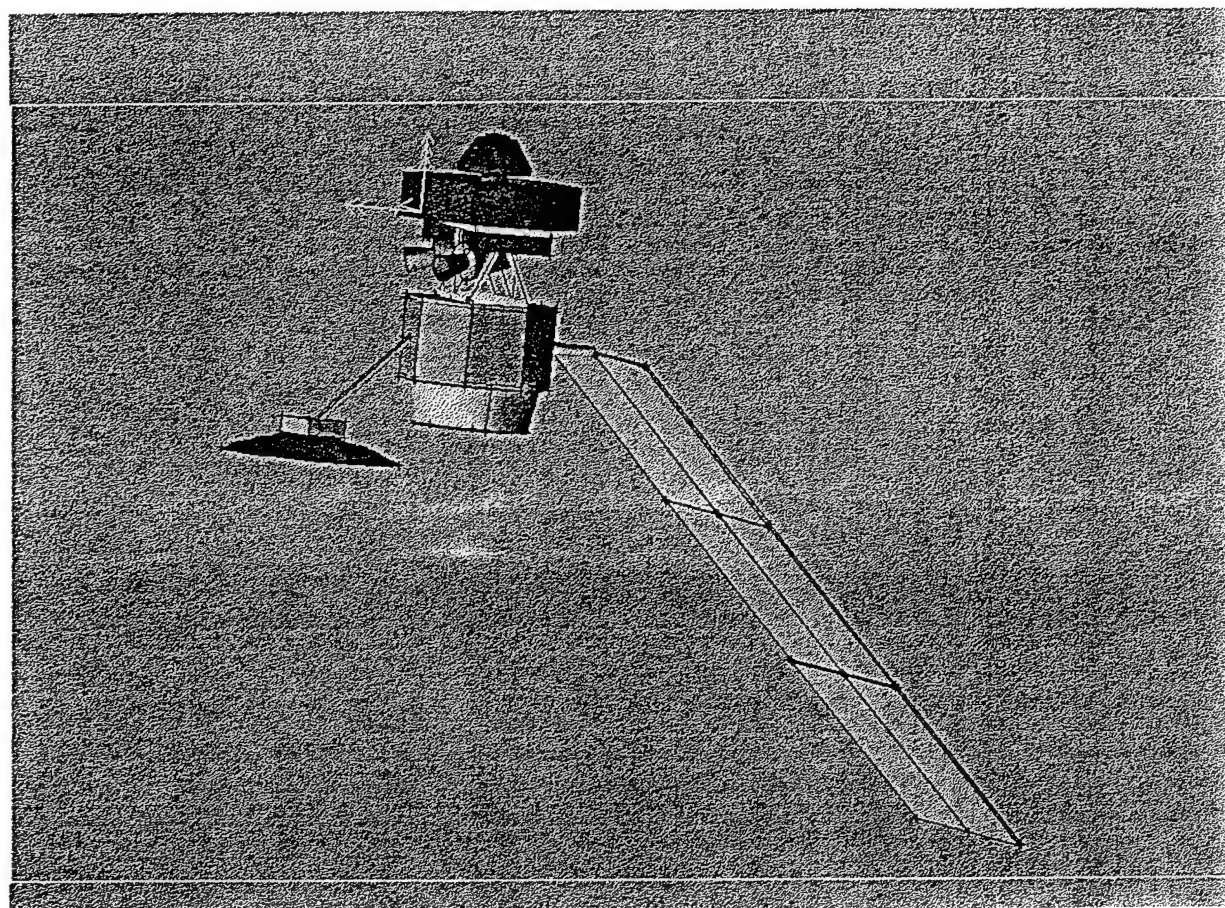
This page was intentionally left blank.

SIMULATION TECHNIQUES

Simulation Techniques

Two simulations were used to analyze the jitter environment of a SmallSat. LEO-SIM and EOS-SIM were both used to evaluate the jitter environment. This allowed direct comparisons of the two simulations and aided in the verification of the results. Each simulation has distinct advantages and disadvantages.

Simulation Techniques

- NASTRAN Finite Element Model

- Low Earth Orbit Simulation (LEO-SIM)

- Platform Simulation (PLATSIM)

Finite Element Modeling

A finite element model of the spacecraft was built using MSC NASTRAN. The NASTRAN model included the spacecraft bus, GLAS experiment, solar array (position corresponding to the ascending node of the spacecraft orbit), and the high gain antenna. The results of the NASTRAN analysis were used as input to both simulations. The spacecraft center of gravity, mass, and mass moments of inertia were used to characterize the SmallSat in LEO-SIM, and the modes and mode shapes were used to describe the rigid body and flexible response of the spacecraft in EOS-SIM.

Finite Element Model

- Modeled the spacecraft bus, GLAS experiment, high gain antenna, and the solar array

- The spacecraft's center of gravity, mass, and mass moments of inertia were used to characterize the spacecraft and payload in LEO-SIM

- The modes and mode shapes were used to define the rigid body and flexible body response of the spacecraft in PLATSIM

Finite Element Modeling

The following tables shows a breakdown of the spacecraft weight and the ACS components:

Spacecraft Weight

Element	Weight (lbs)
DSI Bus (includes ACS)	213.815
GLAS Experiment	108.000
GLAS Telescope	75.700
GLAS Truss	187.600
GLAS Electronics	92.600
GLAS Start Trackers	68.300
Solar Array	80.000
Solar Array Support	0.328
Antenna	10.000
Antenna Support	1.520
Propulsion module	100.000
Stiffeners	0.000
Total	937.863

* Total GLAS Payload weight is 532.2 lbs

ACS Components

Element	Quantity	Weight (lbs)
IMU Electronics	1	6.100
IMU Sensor and Bracket	1	5.200
Horizon Sensor and Bracket	1	6.200
Three Axis Magnetometer	1	0.600
Magnetic Torquer and Bracket	3	16.400
Reaction Wheel and Bracket	4	25.400
ACS Computer	1	11.400
Dual Wheel Driver	2	4.200
Magnetic Torquer Coil and Driver	1	2.200
Total		77.700

* 2 Star Trackers are supplied with the GLAS Payload

The DSI Bus weight includes the spacecraft structure, ACS, power, and data system. The ACS contributes 77.7 pounds to the total weight of the bus.

Finite Element Model

- Mass = 937.8635 lbs.
- Xcg = 0.0 in.
- Ycg = -4.48 in.
- Zcg = 24.28 in.

- Mass Moment of Inertia

I	x	y	z
x	1.06722E+06	7.21882E-13	-2.97688E-14
y	7.21882E-13	7.58682E+05	2.91771E+05
z	-2.97688E-14	2.91771E+05	5.74734E+05

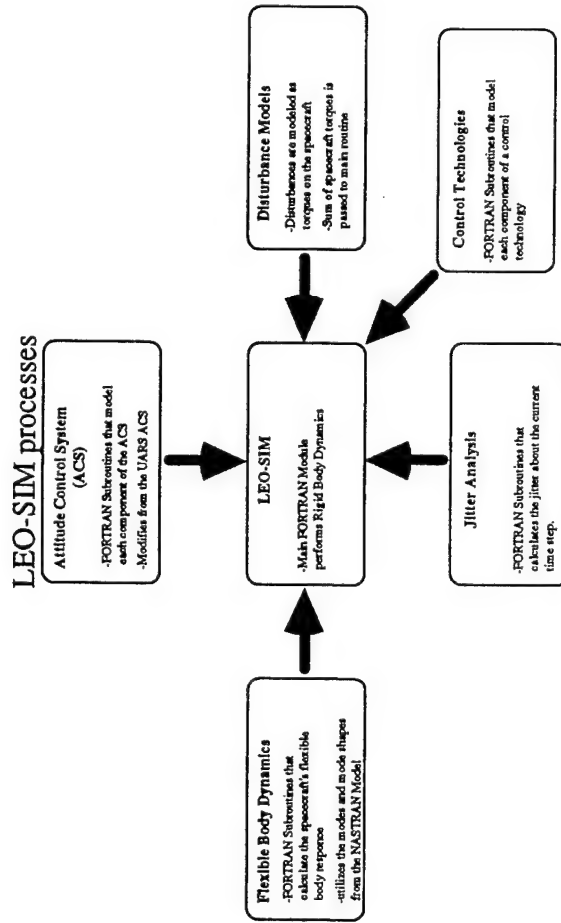This page was intentionally left blank.

Finite Element Model

- Spacecraft natural frequencies with solar array positioned at the ascending node of the orbit

Mode	Frequency (Hz)	Description
1--6	0	Rigid Body Modes
7	0.47314599	Solar Array 1st Bending
8	0.86984300	Solar Array 1st Torsion about support tube
9	1.78894000	Solar Array Torsion about y
10	1.86325000	Solar Array 2nd Bending
11	2.67163990	Solar Array 2nd Torsion about support tube
12	3.29878000	Solar Array Flatwise Bending
13	4.23200000	Solar Array Torsion about support tube
14	4.51895000	Solar Array Bending,Torsion
15	5.12877990	Solar Array Bending,Torsion

LEO-SIM Simulation

The Low Earth Orbit Simulation (LEO-SIM) is a spacecraft simulation initially developed and verified for the UARS platform. The simulation is written in FORTRAN and incorporates rigid body and flexible body responses of a spacecraft. Due to time and resource constraints, only the rigid body response was used for the SmallSat analysis. Few modifications were required to the FORTRAN code for this analysis. Some code was added in order to output jitter calculations and incorporate new disturbance models into the simulation. Most modifications were in the form of changing input parameters that described the spacecraft to be analyzed. The Figure below shows the processes of the LEO-SIM simulation. Torsional forcing functions are used to perturb the model. The simulation will not accept input disturbances in the form of axial forces. Disturbances can be turned on and off at any time in the simulation run. Any global variable can be output and graphed as part of the analysis. Additional FORTRAN subroutines could be written to implement additional controllers for jitter suppression. The LEO-SIM analysis focused on identifying the rigid body jitter environment for each disturbance source.

LEO-SIM processes

Attitude Control System (ACS)
- FORTRAN Subroutines that model each component of the ACS
- Modifies from the UARS ACS

Flexible Body Dynamics
- FORTRAN Subroutines that calculate the spacecraft's flexible body response
- utilizes the modes and mode shapes from the NASTRAN Model

LEO-SIM
- Main FORTRAN Module performs Rigid Body Dynamics

Disturbance Models
- Disturbances are modeled as torques on the spacecraft
- Sum of spacecraft torques is passed to main routine

Control Technologies
- FORTRAN Subroutines that model each component of a control technology

Jitter Analysis
- FORTRAN Subroutines that calculates the jitter about the current time step.

LEO-SIM

- Initially developed and verified for the UARS platform

- Incorporates both rigid body and flexible body responses of the spacecraft (only the rigid body response was analyzed)

- Written in FORTRAN

- Torsional forcing functions are used to perturb the model (simulation will not accept axial forces as input)

- Additional FORTRAN codes could be written to implement additional controllers for jitter suppression

PLATSIM Simulation

The PLATSIM is a spacecraft simulation initially developed and validated for the EOS-AM1 spacecraft. The simulation is written in MATLAB script and incorporates rigid body and flexible body responses of a spacecraft. The spacecraft dynamics are input into the simulation via the modes and mode shapes of the spacecraft determined by the NASTRAN finite element analysis. Both rigid body and flexible body responses were used for the SmallSat analysis using PLATSIM. Few modifications to the code were required for this analysis. Some code was added in order to implement the specific ACS that the SmallSat was to use. Most modifications were implemented when the NASTRAN model of the SmallSat was incorporated into the simulation. The Figure below shows the processes of the PLATSIM simulation. Torsional forcing functions and axial forces are used to perturb the model. Disturbances are changed by modifying the MATLAB script that describes them. Output is restricted to pre-selected parameters. Additional MATLAB script could be written to implement additional controllers for jitter suppression. The SmallSat analysis focused on identifying the jitter environment for each disturbance source.

PLATSIM Processes

42
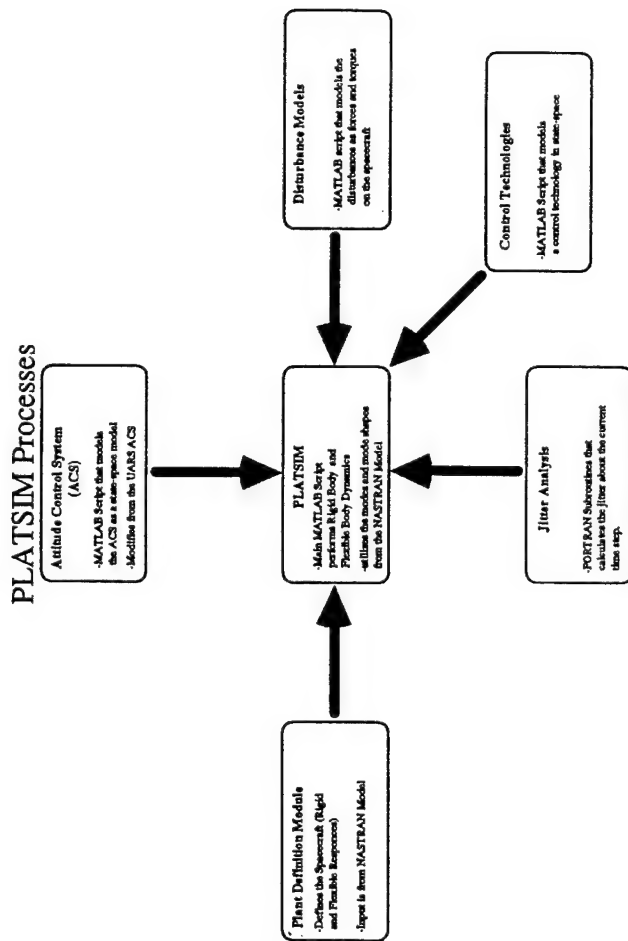
PLATSIM

- Initially developed and validated for EOS-AM-1

- Incorporates both rigid body and flexible body responses of the spacecraft

- Written in MATLAB script

- Spacecraft dynamics are input into the simulation via the modes and mode shapes of the finite element analysis

- Torsional forcing functions and axial forces are used to perturb the model

- Output is restricted to pre-selected parameters

- Additional MATLAB script is available to model controllers for jitter suppression

This page was intentionally left blank.

DISTURBANCES

Disturbances

The SmallSat analysis concentrated on determining the effect of individual disturbances upon the spacecraft. The following disturbances were analyzed: environmental, solar array thermal snap, solar array harmonic drive, and momentum wheel dynamic imbalance. The environmental disturbances are due to solar pressure and aerodynamic forces. The effect of these disturbances upon the SmallSat was derived as a set of forcing functions in roll, pitch, and yaw. Forcing functions are derived as a set of axial forces and torques. Since LEO-SIM does not accept axial forces as input, those forces were transformed to torques by selecting an appropriate moment arm. These forcing functions were used to perturb the simulation.

Disturbances

- The analysis determined the effect of individual disturbances upon the spacecraft

- The following disturbances were studied:
  - environmental
    - aerodynamic
    - solar pressure
  - solar array thermal snap
  - solar array harmonic drive
  - momentum wheel dynamic imbalance
  - high gain antenna (not required by GLAS)
  - cryocooler (not required by GLAS)

Description of the Aerodynamic Disturbance

The model that describes the disturbance on the spacecraft due to aerodynamic forces (drag) was derived from the following equation:

$$T_{aero} = F_{aero} * (C_{pa} - C_g)$$

T_{aero} - Torque on the spacecraft due to aerodynamic forces

F_{aero} - Force on the spacecraft due to aerodynamic forces

C_{pa} - Center of Pressure

C_g - Center of Gravity

$$F_{aero} = -\frac{1}{2}\rho(\frac{C_D A}{m})V^2$$

C_D - Coefficient of drag
m - spacecraft's mass
A - spacecraft's cross sectional area
V - spacecraft's velocity
ρ - atmospheric density

The atmospheric density for this model was derived from the MSIS atmospheric model [Hedin, 1986] with an F10.7 index of 220 (high solar activity). At an altitude of 438 miles (the spacecraft's nominal orbit), the corresponding density is 4.58e-17 slug/ft^3.

Aerodynamic Disturbances

- The aerodynamic disturbance is a function of atmospheric density and vehicle cross sectional area

- The atmospheric density was derived from the Jacchia atmospheric model. An F10.7 index of 220 (high solar activity) was used to predict the worst case

- Aerodynamic torques decrease as altitude increases (air density decreases rapidly)

This page was intentionally left blank.

Aerodynamic Disturbance

Aerodynamic (Roll)

time (sec)

Aerodynamic (Pitch)

time (sec)

Aerodynamic (Yaw)

time (sec)
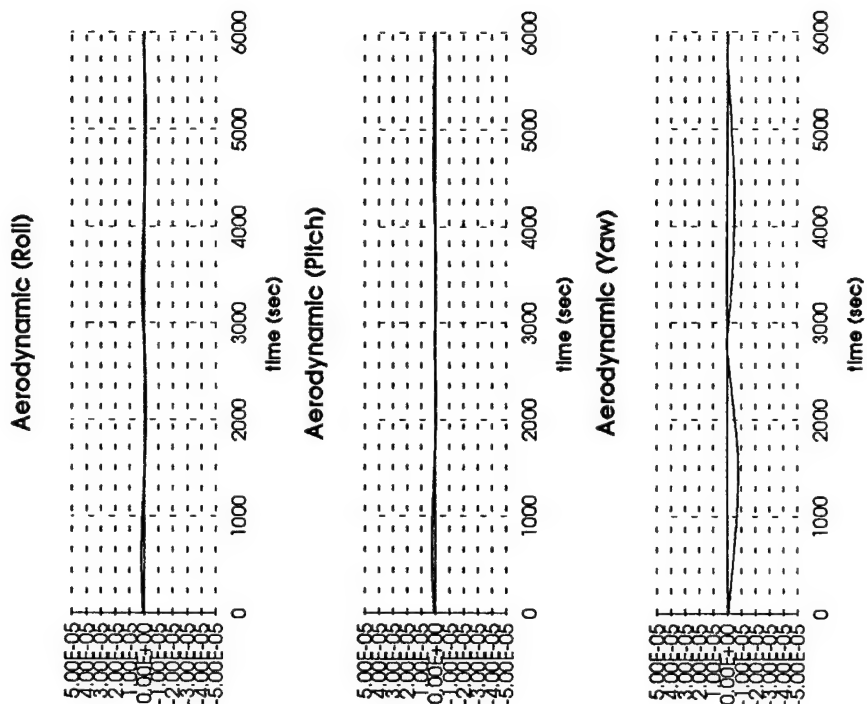
## Description of Solar Pressure Disturbance

The model that describes the disturbance on the spacecraft due to solar pressure torques was derived from the "Solar Activity Inputs for Upper Atmosphere Models," MSFC, 6 April, 1993. The worst case scenario of the solar flux was used to calculate the torque. For this analysis, a launch date of 1/1/95 was assumed.

52

Solar Pressure Disturbances

- Estimate was derived from the "Solar Activity Inputs for Upper Atmospheric Models," MSFC, 6 April, 1993

- Assumed a launch date of 1/1/95

- A worst-case solar flux for this time period was used to calculate the torque

This page was intentionally left blank.

Solar Pressure Disturbance

Solar Pressure (Roll)

Solar Pressure (Pitch)

Solar Pressure (Yaw)
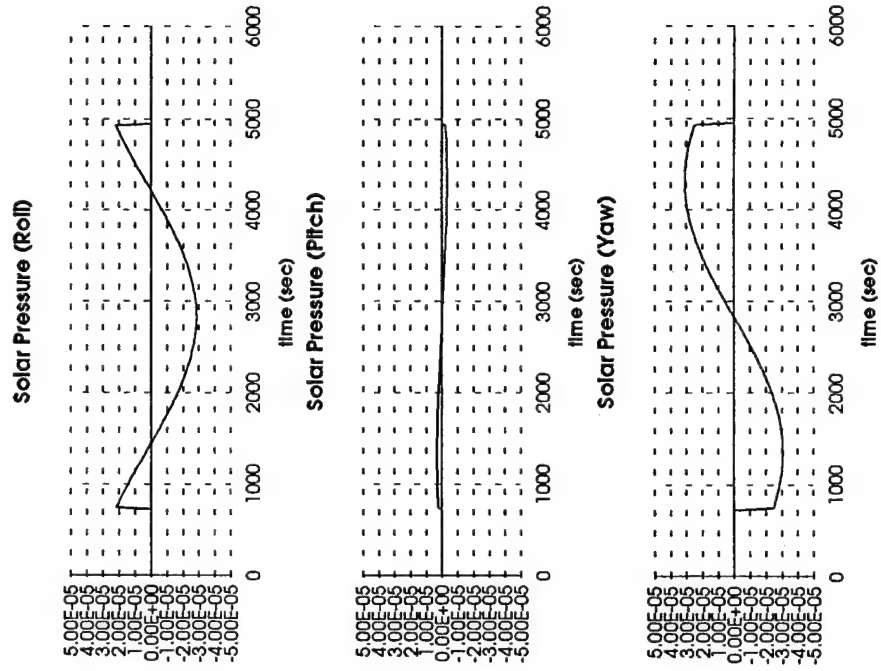
Thermal Snap

The model of the disturbance caused by the thermal snap of the solar array as it enters and leaves the penumbra is based upon a similar analysis performed for the UARS solar array. For this type of an array, the thermal snap is more of a bending phenomena.

Description of Thermal Snap Disturbance

The forcing function which describes the torsional disturbance caused by the thermal snap of the solar array is calculated as follows:

$$\text{TROLL} = -\text{Tn} * \text{COS}(\text{PANG} * \frac{2\pi}{360})$$

$$\text{TPITCH} = 0$$

$$\text{TYAW} = \text{Tn} * \text{SIN}(\text{PANG} * \frac{2\pi}{360})$$

Tn - Torque normal to the solar array (ft lb)
PANG - Angle that the normal of the solar array makes with the sun (degrees)

The torque normal to the solar array surface due to thermal snap (T_n) is calculated as follows:

The Torque normal to the solar array panel can be expressed as follows:

$$T_n = \frac{T_{mag} * t_d}{t_r * (t_p - t_r)} * (sign + FAC)$$

Tmag - Magnitude of the reference torque (ft lb)
t_d - decay time of exponential function (sec)
t_r - rise time (sec)

t_p - time spent in penumbra (sec)

The values for SIGN and FAC are defined on the next facing page. A full derivation of the thermal snap disturbance will be included in an AIAA paper authored by T. Johnson and C. Nguyen by July 1994.

Thermal Snap Disturbance

- Estimate of disturbance torque was based on the thermal snap analysis performed for UARS

- The following parameters were modified to correct for changes in the spacecraft

  - Panel dimensions
  - Spacecraft altitude
  - Location of the sun (beta angle)

- Net effect changed magnitude of the torque normal to the solar array from 0.005 ft lbs to 0.0017 ft lbs

- The torque occurs over a short period (100 sec) when the spacecraft enters and leaves the penumbra

Description of Thermal Snap Disturbance (Continued)

The values for SIGN and FAC are defined for each time interval as follows:

$[0 < t < t_r]$

$$FAC = -EXP\left(\frac{-t}{t_a}\right)$$

$$SIGN = 1$$

$[t_r < t < (t_p - t_r)]$

$$FAC = -EXP\left(\frac{-t}{t_a}\right) + EXP\left(\frac{-(t - t_r)}{t_a}\right)$$

$$SIGN = 0$$

$[(t_p - t_r) < t < t_p]$

$$FAC = -EXP\left(\frac{-t}{t_a}\right) + EXP\left(\frac{-(t - t_r)}{t_a}\right) + EXP\left(\frac{-(t - t_p + t_r)}{t_a}\right)$$

$$SIGN = -1$$

$[t_p < t]$

$$FAC = -exp\left(\frac{-t}{t_a}\right) + exp\left(\frac{-(t - t_r)}{t_a}\right) + exp\left(\frac{-(t - t_p + t_r)}{t_a}\right) - exp\left(\frac{-(t - t_p)}{t_a}\right)$$

$$SIGN = 0$$

Thermal Snap Disturbance

High Gain Antenna (HGA)

The model of the disturbance caused by the return sweep of the high gain antenna is taken directly from the collaborative study between the Goddard Space Flight Center (GSFC) and the Langley Research Center (LaRC) that investigated the application of Control-Structure Integration technologies to the EOS AM-1 spacecraft. The model was developed from information supplied by the "T9: A4 Internal Disturbances Document" and reviewed by the pointing performance team consisting of GSFC, LaRC, McDonnell Douglas, Martin Marietta, and Swales and Associates, Inc.

The HGA has a elevation and azimuth gimbal that produce torques on the spacecraft. The azimuth scan produces a torque about the z axis. The torque profile is a rectangular pulse with magnitude of 0.002667 in-lbf and period of 290 seconds.
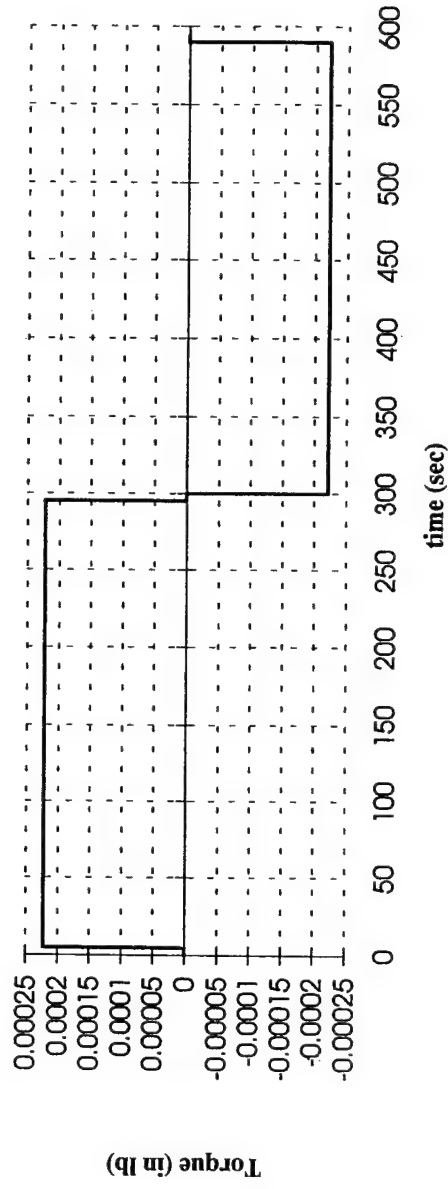
High Gain Antenna Disturbance

- Estimate of disturbance torque was based on the analysis performed for EOS

- Disturbance due to the antenna's azimuth gimbal (the model does not include tracking and dithering of the antenna)

- Disturbance torque is a pulse in the spacecraft's yaw axis

- The torque occurs over a short period (600 sec) when the antenna sweeps to capture the next relay satellite

This page was intentionally left blank.

High Gain Antenna Disturbance

High Gain Antenna Disturbance (Yaw)

Torque (in lb)

0.00025
0.0002
0.00015
0.0001
0.00005
0
-0.00005
-0.0001
-0.00015
-0.0002
-0.00025

0 50 100 150 200 250 300 350 400 450 500 550 600

time (sec)

Momentum Wheel Dynamic Imbalance Model

The model that describes the disturbance caused by a dynamic imbalance of the momentum wheels is based upon measured values of similar momentum wheels. Momentum wheel imbalances are measured for each half of the wheel and are characterized as a point mass at a specific radius. The momentum wheels were modeled after the momentum wheels used by the COMET ACS. Typical imbalances for the COMET momentum wheels are characterized as a 25 mg point mass at a 1 inch radius for each half of the wheel. For our analysis, the momentum wheel imbalance was modeled as a single 50 mg point mass at a 1 inch radius. The following Figure displays the model of the momentum wheel dynamic imbalance.

Model of a Dynamic Imbalance of a Momentum Wheel
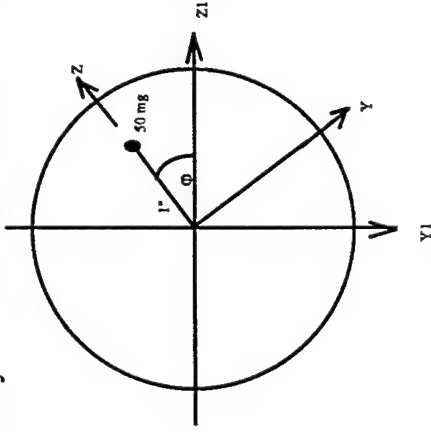
Momentum Wheel Dynamic Imbalance Disturbance

- A momentum wheel package similar to the package used on COMET was selected

- Imbalances for each half of the COMET wheels were measured and characterized as a 25 mg point mass at a 1 inch radius

- The wheel imbalance was modeled as one 50 mg point mass at a 1 inch radius

- Applied the imbalance to the roll-axis momentum wheel

- The torque due to the wheel imbalance is a function of the wheel speed, which changes through the spacecraft's orbit, and the wheel location

Description of Momentum Wheel Dynamic Imbalance Disturbance

The forcing function that describes the disturbance caused by the dynamic imbalance of the momentum wheel is calculated as a function of the mass and position of a point mass and the speed that the wheel is rotating. For EOS-SIM, this disturbance is represented as an axial force due to the angular acceleration of the point mass. For LEO-SIM, the force is coupled with a moment arm to produce a torque. This is done because LEO-SIM does not allow for axial forces as input. The force (F) due to the centrifugal acceleration of the point mass is calculated as follows:

$$F_x = 0$$
$$F_Y = 0$$
$$F_z = m\omega^2 r$$

F - centrifugal acceleration due to the point mass in (X,Y,Z) reference frame (lb)
m - mass of the point mass (slugs)
r - radius of point mass from center of the momentum wheel (ft)
ω - wheel's angular velocity (Hz)

The wheel's angular velocity is calculated as follows:

$$\omega = \frac{H}{I}$$

ω - wheel's angular velocity (Hz)
H - wheel's angular momentum (ft lb sec)

I - wheel's inertia (slug ft^2)

The force (F) is transformed from a reference frame that is fixed to the rotating wheel to the spacecraft reference frame. For LEO-SIM, the force is transformed to a torque by selecting an appropriate moment arm.

Momentum Wheel Dynamic Imbalance Disturbance
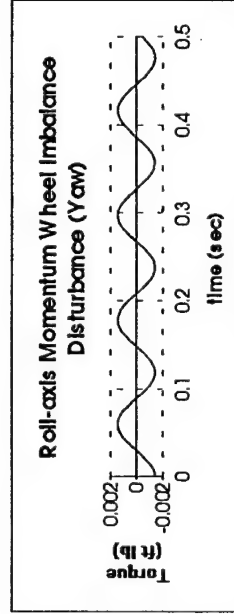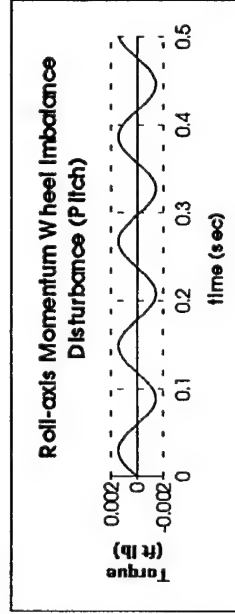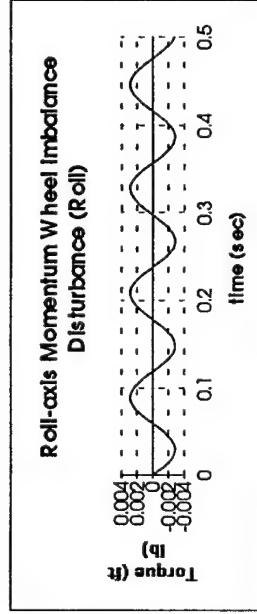
Solar Array Harmonic Drive Model

The model of the disturbance caused by the solar array harmonic drive is based upon a similar analysis performed for the EOS and UARS harmonic drives. For the analysis, it was assumed that the solar array rotates at a constant rate and that the torque variations induced on the spacecraft by the harmonic drive are sinusoidal. For this analysis, we assumed the parameters of the harmonic drive were equal to those for the UARS harmonic drive. We chose the UARS harmonic drive because it has a higher disturbance frequency and less of an impact on the spacecraft than the EOS harmonic drive. The following Figure depicts the model of the solar array harmonic drive.

Model of the Solar Array Harmonic Drive
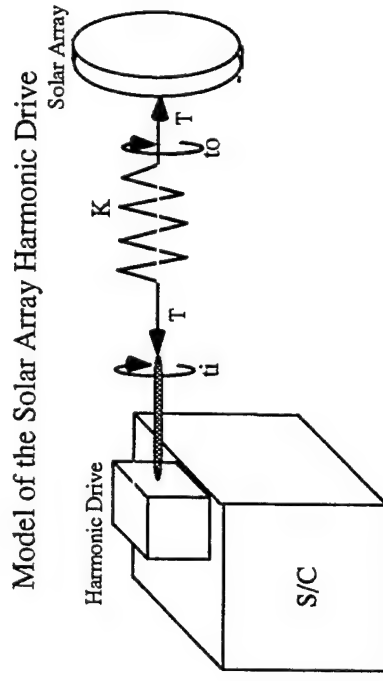
Solar Harmonic Drive Disturbance

- Estimate of disturbance torque was based on the analysis performed for EOS and UARS

- Assumed that the solar array rotates at a constant rate and the torque variations are sinusoidal

- Assumed the parameters of the harmonic drive were equal to those for the UARS harmonic drive

- Adjusted the magnitude of the torque based on the reduced size of the solar array

- The UARS harmonic drive produces a higher frequency disturbance torque (had a smaller impact on the spacecraft)

Description of Solar Array Harmonic Drive Disturbance

The forcing function which describes the torsional disturbance of the solar array harmonic drive is represented by a magnitude (T_{HD}) and a frequency (w_{HD}). The position error of the harmonic drive is characterized by the following equation:

$$\Delta\theta = \frac{4}{PD*GR} * \frac{2\pi}{360}$$

$\Delta\theta$ - Drive position error (rad); difference between actual and desired position

GR - gear ratio of the harmonic drive (non-dimensional)

PD - (non-dimensional)

The torsional disturbance results from a periodic position error of the harmonic drive. The magnitude of the harmonic drive disturbance is calculated as follows:

$$T_{HD} = K * \Delta\theta$$

$$where$$

$$K = J * \omega_{SA}^2$$

K - Stiffness associated with the solar array (ft lb/rad)

J - Solar array inertia (slug ft^2)

ω_{sa} - Solar array torsion frequency (rad/sec)
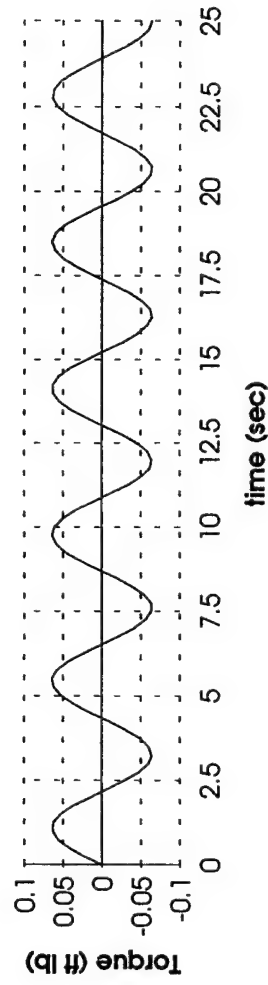
The frequency of the harmonic drive disturbance is calculated as follows:

$$\omega_{HD} = 2 * \left(RPM * \frac{1 \text{ min}}{60 \text{ sec}} \right)$$

ω_{HD} - Frequency of the harmonic drive disturbance (Hz)

RPM - input RPM of the harmonic drive (rev/min)

Solar Harmonic Drive Disturbance

Harmonic Drive Disturbance (Pitch)

Cryocooler

The model of the disturbance caused by the cryocooler is taken directly from the collaborative study of the MOPITT Cryocooler disturbance between the Goddard Space Flight Center (GSFC) and the Langley Research Center (LaRC) that investigated the application of Control-Structure Integration technologies to the EOS AM-1 spacecraft. The model was developed from information supplied by the instrument principal investigators and reviewed and agreed upon by the pointing performance team consisting of GSFC, LaRC, McDonnell Douglas, Martin Marietta, and Swales and Associates, Inc.

The MOPITT cryocooler has a compressor and displacer that produce forces and torques on the spacecraft. The cryocooler compressor produces forces in the y and x directions and a torque in the pitch axis. These forces and torques act at frequencies of 46, 92, and 138 Hz. The cryocooler displacer produces forces in the y and x (or z) and a torque in the pitch axis. Again, the forces and torques act at 46, 92, and 138 Hz.

Cryocooler Disturbance

- Estimate of disturbance torque was based on the analysis performed for EOS

- Model was not changed from the one presented in the "Evaluation of CSI Enhancements for Jitter Reduction on the EOS AM-1 Spacecraft", NASA/LaRC CSIO Memorandum 93-09-01

- Cryocooler compressor and displacer disturbances were analyzed (disturbance frequencies at 46, 92, and 138 Hz)

This page was intentionally left blank.

Cryocooler Disturbance
(Compressor)

MOPITT Cryocooler Compressor (Roll Force)

Force (lb)

1.50E-01
1.00E-01
5.00E-02
0.00E+00
-5.00E-02
-1.00E-01
-1.50E-01

0   0.025   0.05   0.075   0.1   0.125   0.15

time (sec)

MOPITT Cryocooler Compressor (Pitch Force)

Force (lb)

1.50E-01
1.00E-01
5.00E-02
0.00E+00
-5.00E-02
-1.00E-01
-1.50E-01

0   0.025   0.05   0.075   0.1   0.125   0.15

time (sec)

MOPITT Cryocooler Compressor (Pitch Torque)

Torque (ft lb)

3.00E-01
0.00E+00
-3.00E-01

0   0.025   0.05   0.075   0.1   0.125   0.15

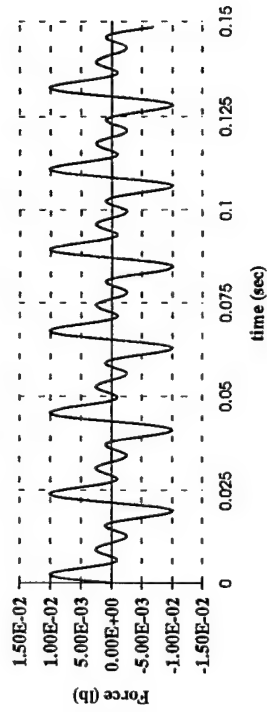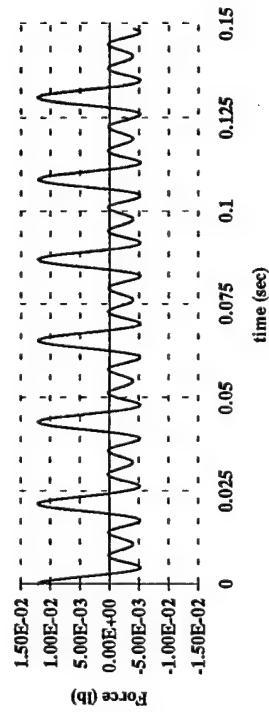time (sec)
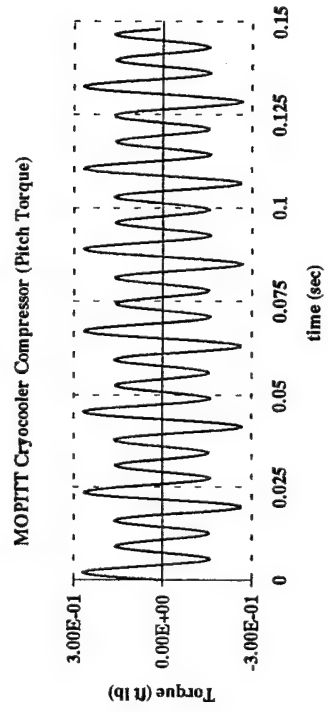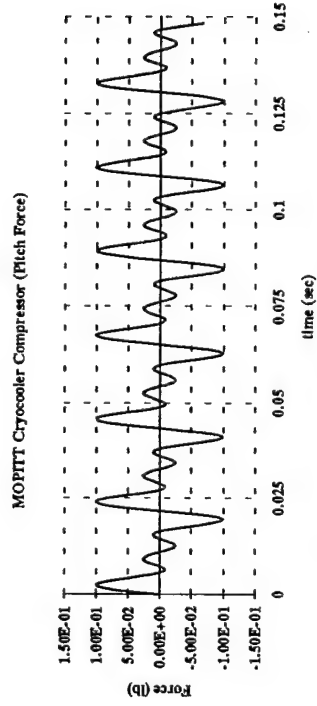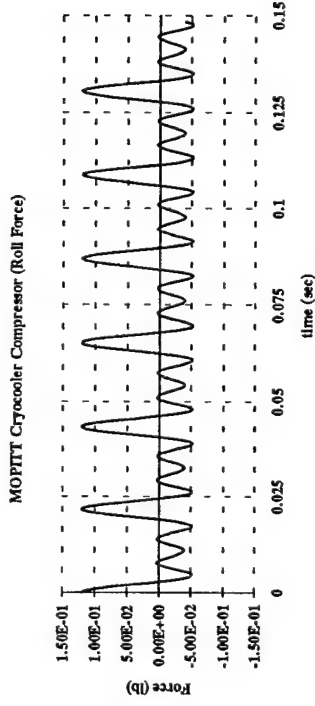
This page was intentionally left blank.

Cryocooler Disturbance
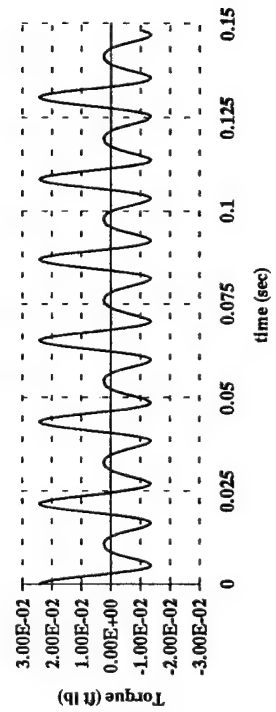## (Displacer)

MOPITT Cryocooler Displacer (Roll Force)

MOPITT Cryocooler Displacer (Pitch Force)

MOPITT Cryocooler Displacer (Pitch Torque)

This page was intentionally left blank.

ANALYSIS RESULTS

Summary of Results

The results of the SmallSat simulations show that a payload requirement of 2 arcsec/sec for both rigid body and flexible body analysis is not satisfied by the generic satellite used for this study. The results of the SmallSat simulation are listed by the amount of jitter that the disturbance produces (largest to the smallest). Three disturbances exceed the payload jitter requirement of 2 arcsec/sec by themselves: the solar array harmonic drive, the thermal snap of the solar array when the array enters and leaves the penumbra, and the return sweep of the high gain antenna. The solar array harmonic drive accounted for the most jitter (approximately 50 arcsec/sec in pitch and 30 arcsec/sec in yaw). The next largest disturbances were the thermal snap of the solar arrays, and the return sweep of the high gain antenna (on the order of 5 arcsec/sec). The jitter associated with thermal snap is negligible except for 150 seconds when the spacecraft enters and leaves the penumbra. The smallest disturbances were the cryocooler and the dynamic imbalance of the roll-axis momentum wheel (on the order of 1 arcsec/sec). For this spacecraft, the jitter associated with the pitch and yaw-axis momentum wheels will not exceed the jitter of the roll-axis momentum wheel. The jitter associated with the environmental disturbances is also negligible.

Results

- The payload requirement of 2 arcsec/sec is not satisfied by the generic satellite used for this study

- Jitter due to Environmental disturbances was negligible

- Three disturbances (harmonic drive, thermal snap, and high gain antenna) exceeded the requirement by themselves

- The worst offender was the solar array harmonic drive (Jitter associated with the solar array harmonic drive must be reduced by two orders of magnitude)

- Jitter associated with thermal snap and the high gain antenna must be reduced by one order of magnitude

This page was intentionally left blank.

Results

Disturbance/	Jitter (arcsec/sec)		
Simulation	Roll	Pitch	Yaw
Solar Array Harmonic Drive			
LEO-SIM	0.03	52.00	0.10
EOS-SIM (Rigid Body)	0.00	60.03	30.08
EOS-SIM (50 Modes)	0.00	59.60	30.12
Solar Array Thermal Snap			
LEO-SIM	4.00	0.00	7.80
EOS-SIM (Rigid Body)	2.55	0.02	0.07
EOS-SIM (50 Modes)	2.54	0.02	0.07
High Gain Antenna Return Sweep			
LEO-SIM	0.50	0.08	5.00
EOS-SIM (Rigid Body)	0.00	1.69	6.96
EOS-SIM (50 Modes)	0.00	1.69	6.96
Cryocooler			
EOS-SIM (Rigid Body)	0.32	0.46	0.68
EOS-SIM (50 Modes)	0.67	0.65	0.90
Momentum Wheel Dynamic Imbalance			
LEO-SIM	0.04	0.70	0.07
EOS-SIM (Rigid Body)	0.05	0.06	0.07
EOS-SIM (50 Modes)	0.14	0.09	0.14

This page was intentionally left blank.

Solar Array Harmonic Drive Jitter Time History

(from EOS-SIM with all 50 modes
and control system on @ 0.07 rad/sec bandwidth)
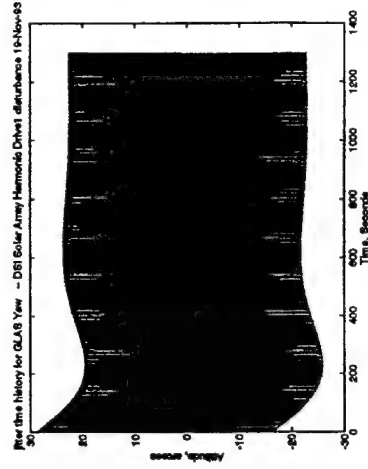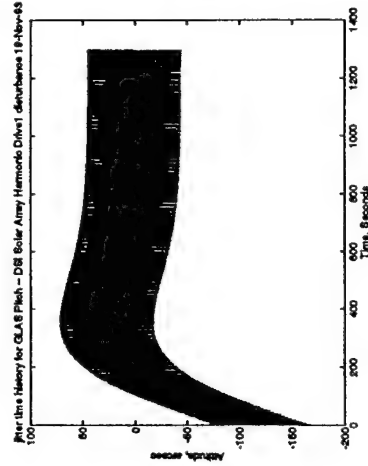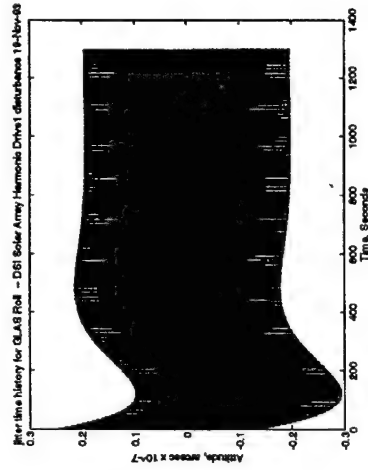
This page was intentionally left blank.

High Gain Antenna Jitter Time History

(from EOS-SIM with all 50 modes
and control system on @ 0.07 rad/sec bandwidth)
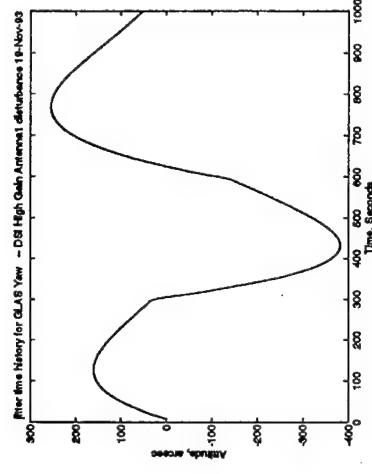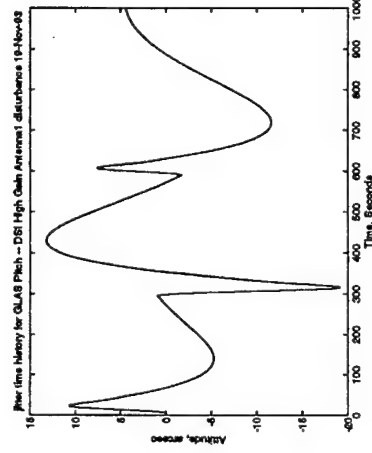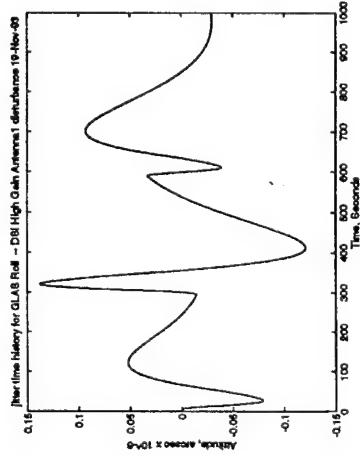
This page was intentionally left blank.

Solar Array Thermal Snap Jitter Time History

(from EOS-SIM with all 50 modes and control system on @ 0.07 rad/sec bandwidth)
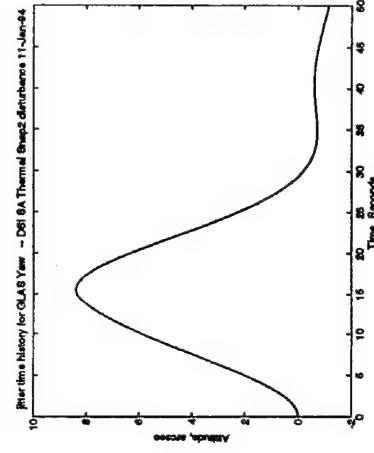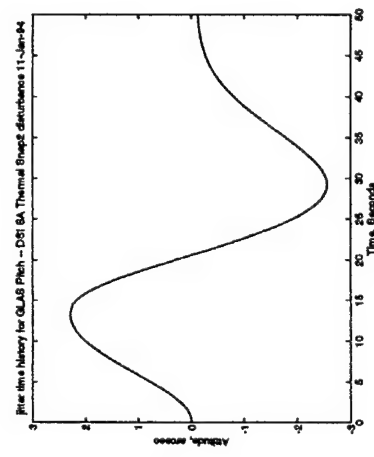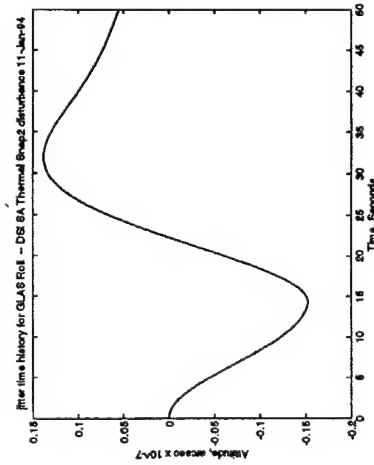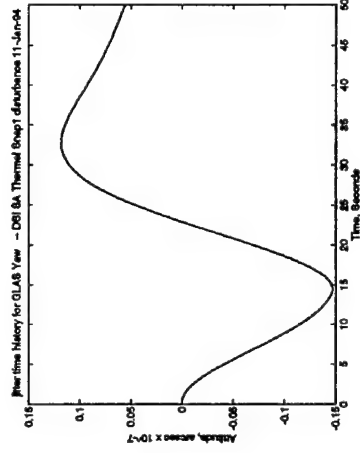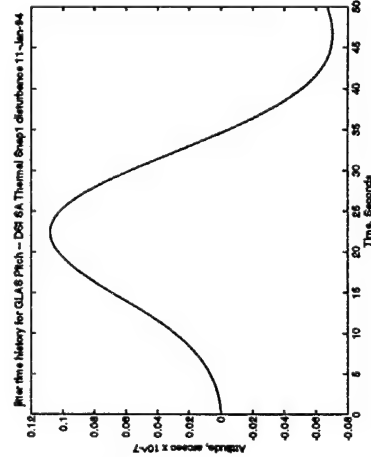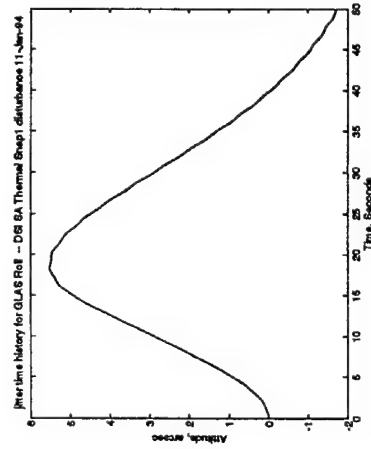
This page was intentionally left blank.

CONCLUSIONS

Conclusions

This study shows the importance of identifying and quantifying on-board vibrational disturbances associated with operating machinery and flight dynamics. Even with a simple hardware configuration, on-board disturbances can exceed payload jitter requirements and reduce instrument science return. Over time, spacecraft buses and payloads have become smaller in size due to advances in microelectronics, however, mechanical devices have not matured as rapidly. Devices (e.g., pumps, gimbals, fans) that are normally associated with large mission masses (e.g., UARS, EOS, HST), are now being proposed for SmallSats. The disturbances associated with these components will contribute more significantly to SmallSats as there is less inertia to overcome when the component induces vibration.

The selection of quiet hardware should be considered for spacecraft designs. There appears, however, that even with the best designs and the quietest equipment, the science objectives of current and proposed imaging sensors may conflict with the engineering capability of the best hardware. These investigators have concluded that active control technologies will be needed to fill this gap for some future remote sensing missions. Control technologies have the potential to enhance existing hardware performance and image resolution, and can create opportunities that otherwise would have been unavailable.

Conclusions

- This type of analysis is needed to address vibration issues when designing remote sensing payloads

- Hardware routinely used on large spacecraft may be unacceptable for SmallSats

- SmallSats outfitted with vibration monitoring instruments would greatly add to the understanding of SmallSat jitter

- Control Technologies may be useful (and in some cases essential) in jitter reduction for SmallSats

This page was intentionally left blank.

Reference

1. 1993 EOS Reference Handbook, March 1993.

This page was intentionally left blank.

APPENDICES

This page was intentionally left blank.

APPENDIX A -- EOS INSTRUMENT RESOURCE REQUIREMENTS

Instrument Name	Acronym	Flight Assignment	Mass (kg)	Mass (lb)	Thermal Range (C)	Power (Watts) Avg.	Peak	Data Rate (kbps) Avg.	Peak
Earth Observing Scanning Polarimeter	EOSP	AM	19	42	0 -- 40	14	22	44	88
Lightning Imaging Senor	LIS	TRMM1	20	44	0 -- 40	33	33	6	6
Solid State Altimeter	SSALT	ALT	25	55	(-5) --35	49	49	1.375	11.5
Active Cavity Radiometer Irradiance Monitor	ACRIM	CHEM	39	86	10 -- 30	35	40	1	1
Stratospheric Aerosol and Gas Experiment	SAGE III	AERO	40	88	10 -- 30	15	60	100	100
Doppler Orbitography and Radiopositioning Integrated by Satellite	DORIS	ALT	44	97	(-10) -- 50	17.6	17.6	0.03125	0.03125
TOPEX Microwave Radiometer	TMR	ALT	50	110	5 -- 40	26	26	0.125	0.125
Microwave Humidity Sounder	MHS	PM	66	146	0 -- 40	85	190	4.2	4.2
Clouds and Earth's Radiant Energy System	CERES	AM/PM	90	198	(-15) --39	95	171	20	20
Solar Stellar Irradiance Comparison Experiment	SOLSTICE II	CHEM	100	220	0 -- 30	34	42	5	8
Advanced Microwave Sounding Unit	AMSU	PM	100	220	0 -- 20	125	125	3.2	3.2
Multi-Angle Imaging SpectroRadiometer	MISR	AM	106	234	(-20) -- 40	67	107	3800	6500
Measurements of Pollution in the Troposphere	MOPITT	AM	120	265	25	200	200	6	6
Geoscience Laser Altimeter System	GLAS	ALT	125	276	0 -- 25	175	175	<200	<200
Atmospheric Infrared Sounder	AIRS	PM	140	309	20 -- 25	224	224	1420	1420
High-Resolution Dynamics Limb Sounder	HIRDLS	CHEM	150	331	20 -- 30	180	230	40	40
Moderate-Resolution Imaging Spectroradiometer	MODIS-T	AM/PM	170	375	0 -- 40	130	155	3076	3076
Multifrequency Imaging Microwave Radiometer	MIMR	PM	223	492	(-10) -- 50	171.4	200	67	67
Moderate-Resolution Imaging Spectrometer-Nadir	MODIS-N	AM/PM	250	551	0 -- 40	225	275	6200	11000
NASA Scatterometer	NSCAT II	ADEOS II	270	595	5 -- 50	290	290	5.1	5.1
Tropospheric Emission Spectrometer	TES	AM	340	750	0 -- 30	430	460	3240	19500
Advanced Spaceborne Thermal Emission and Reflection Radiometer	ASTER-VNIR	AM	400	882	10 -- 28	449	674	8300	89200
Advanced Spaceborne Thermal Emission and Reflection Radiometer	ASTER-SWIR	AM	400	882	10 -- 28	449	674	8300	89200
Advanced Spaceborne Thermal Emission and Reflection Radiometer	ASTER-TIR	AM	400	882	10 -- 28	449	674	8300	89200
Microwave Limb Sounder	MLS	CHEM	500	1102	10 -- 35	540	540	5	5
EOS-COLOR	EOS-COLOR	COLOR	TBD	TBD	TBD	TBD	TBD	TBD	TBD

Source: EOS Reference Handbook, May 1993

APPENDIX A -- EOS INSTRUMENT RESOURCE REQUIREMENTS

Instrument Name	Acronym	Flight Assignment	Mass (kg)	Mass (lb)	Thermal Range (C)	Power (Watts) Avg.	Peak	Data Rate (kbps) Avg.	Peak
Ionospheric Plasma and Electrodynamics Instrument	IPEI	NONE	12	26	(-10) -- 50	10	10	1.1	1.1
GPS Geoscience Instrument	GGI	NONE	60	132	10 -- 20	105	105	50	50
X-ray Imaging Experiment	XIE	NONE	71	157	(-50) -- (-20)	21	34	5	10
Geomagnetic Observing System	GOS	NONE	96	212	(-10) -- 40	67.3	67.3	20	20
Stratospheric Wind Infrared Limb Sounder	SWIRLS	NONE	150	331	TBD	250	270	3	3
Altimeter	ALT	NONE	275	606	0 -- 35	232	250	80	80
Stick Scatterometer	STIKSCAT	NONE	297	655	5 -- 50	290	290	5.2	5.2
Geoscience Laser Ranging System	GLRS	NONE	350	772	15 -- 25	450	660	400	800
Spectroscopy of the Atmosphere using Far Infrared Emissions	SAFIRE	NONE	407	897	(-10) -- 30	465	465	8700	8700
High-Resolution Imaging Spectrometer	HIRIS	NONE	450	992	0 -- 40	300	600	3000	100000
Laser Atmospheric Wind Sounder	LAWS	NONE	800	1764	TBD	2200	TBD	2000	10000
EOS Synthetic Aperture Radar	EOS SAR	NONE	1100	2425	TBD	1600	5800	15000	180000

APPENDIX A (cont.)

Instrument Name	Placement (arcsec)			Knowledge (arcsec)			Stability (arcsec/sec)			Jitter (arcsec/sec)		
	Roll	Pitch	Yaw	Roll	Pitch	Yaw	Roll	Pitch	Yaw	Roll	Pitch	Yaw
EOSP	3600	3600	3600	150	150	150	100/10	100/10	100/10	100/10	100/10	100/10
LIS	none	none	none	293	293	293	TBD	TBD	TBD	TBD	TBD	TBD
SSALT	720	720	720	360	360	360	TBD	TBD	TBD	TBD	TBD	TBD
ACRIM	360	360	360	180	180	180	360	360	360	360	360	360
SAGE III	3600	3600	3600	900	900	900	30	30	30	TBD	TBD	TBD
DORIS	5400	5400	5400	720	720	720	TBD	TBD	TBD	TBD	TBD	TBD
TMR	1080	1080	1080	1800	1800	1800	1800	1800	1800	1800	1800	1800
MHS	3600	3600	3600	360	360	360	74	74	74	TBD	TBD	TBD
CERES	720	720	720	180	180	180	79/6.6	79/6.6	79/6.6	TBD	TBD	TBD
SOLSTICE II	±360	±360	±360	60	60	60	15/900	15/900	15/900	15	15	15
AMSU	720	720	720	360	360	360	360	360	360	360	360	360
MISR	240	240	240	108	108	108	16/420	16/420	16/420	7/1	7/1	7/1
MOPITT	500	500	500	500	500	500	322/12.47	322/12.47	322/12.47	TBD	TBD	TBD
GLAS	90	90	90	5	5	5	2	2	2	<2	<2	<2
AIRS	900	900	900	900	900	900	360/60	360/60	360/60	TBD	TBD	TBD
HIRDLS	900	900	900	250	250	250	30	30	30	TBD	TBD	TBD
MODIS-T	3600	3600	3600	141	141	141	28	28	28	1031	47	1031
MIMR	720	720	720	108	108	108	36	36	36	TBD	TBD	TBD
MODIS-N	3600	3600	3600	141	141	141	28	28	28	1031	47	1031
NSCAT II	324	324	324	216	216	216	396/1800	396/1800	396/1800	TBD	TBD	TBD
TES	108	108	108	108	108	108	36	36	36	TBD	TBD	TBD
ASTER-VNIR	293	293	293	123	123	123	8.8	8.8	15	8.8	4.4	52
ASTER-SWIR	293	293	293	123	123	123	8.8	8.8	15	8.8	4.4	52
ASTER-TIR	293	293	293	123	123	123	8.8	8.8	15	8.8	4.4	52
MLS	1800	1800	1800	180	180	180	100/30	100/30	100/30	10/0.5	10/0.5	10/0.5
EOS-COLOR	TBD	TBD	TBD	293	293	293	TBD	TBD	TBD	TBD	TBD	TBD

Source: EOS Reference Handbook, May 1993

APPENDIX A (cont.)

Instrument Name	Placement (arcsec)		Knowledge (arcsec)			Stability (arcsec/sec)			Jitter (arcsec/sec)		
	Pitch	Yaw	Roll	Pitch	Yaw	Roll	Pitch	Yaw	Roll	Pitch	Yaw
IPEI	1800	1800	360	360	360	3600	3600	3600	360	360	360
GGI	3600	3600	123	123	123	TBD	TBD	TBD	TBD	TBD	TBD
XIE	3600	3600	3600	3600	3600	3600	3600	3600	3600	3600	3600
GOS	TBD	TBD	10	10	10	N/A	N/A	N/A	N/A	N/A	N/A
SWIRLS	2700	3900	120	60	36	1.3	1.3	1.3	TBD	TBD	TBD
ALT	TBD	TBD	TBD	TBD	TBD	TBD	TBD	TBD	TBD	TBD	TBD
STIKSCAT	324	324	216	216	216	396/1800	396/1800	396/1800	TBD	TBD	TBD
GLRS	90	90	10	10	10	TBD	TBD	TBD	TBD	TBD	TBD
SAFIRE	750	750	10	10	10	1/9.0	1/9.0	1/9.0	TBD	TBD	TBD
HIRIS	293	293	117	117	117	1.08	1.08	1.08	7.2/1000	7.2/1000	7.2/1000
LAWS	36	36	TBD	TBD	TBD	7.2/1000	7.2/1000	7.2/1000	1	1	1
EOS SAR	30	30	3	3	3	0.6	0.6	0.6	TBD	TBD	TBD

Source: EOS Reference Handbook, May 1993

APPENDIX A (cont.)

Instrument Name	Stowed Dimension (cm.)			Deployed Dimension (cm.)		
	Length	Width	Height	Length	Width	Height
EOSP	51	26	81	51	56	81
LIS	30	20	30	30	20	30
SSALT	36.5	28.8	23.2	36.5	28.8	23.2
ACRIM	38	14	18	38	14	18
SAGE III	25	25	42	34	74	-
DORIS	33	35	21	39	32	21
TMR	35	51	61	30	91	-
MHS	77.4	99	56	77.4	99	56
CERES	60	60	57.6	60	60	70
SOLSTICE II	121	88	61	121	88	61
AMSU	65.5	29.9	59.2	65.5	29.9	59.2
MISR	127	78	92	127	78	92
MOPITT	102.9	72.9	43.6	102.9	75.1	43.6
GLAS	100	100	80	100	100	80
AIRS	116.5	80	95.3	116.5	158.7	95.3
HIRDLS	130	80	100	130	90	120
MODIS-T	140	125	56	140	125	87
MIMR	180	170	130	300	170	170
MODIS-N	95.2	158.3	133.6	95.2	158.3	133.6
NSCAT II	122	91	25	318	91	25
TES	140	130	100	220	130	100
ASTER-VNIR	53.8	65.1	83.2	53.8	65.1	83.2
ASTER-SWIR	73	124	95	73	124	95
ASTER-TIR	54	140	120	54	140	120
MLS	160	180	160	160	180	160
EOS-COLOR	TBD	TBD	TBD	TBD	TBD	TBD

APPENDIX A (cont.)

EOS Instrument	Stowed Dimension (cm)			Deployed Dimension (cm)		
	Length	Width	Height	Length	Width	Height
IPEI	25	41	39	25	41	39
GGI	20.32	30.48	38.1	-	-	-
XIE	20	120	20	20	120	20
GOS	80	160	30	24	65	29
SWIRLS	160	140	120	160	140	120
ALT	TBD	TBD	TBD	TBD	TBD	TBD
STIKSCAT	122	91	25	122	91	25
GLRS	150	150	95	150	150	95
SAFIRE	160	160	160	160	160	160
HIRIS	86	33	86	86	33	86
LAWS	-	160	160	-	160	160
EOS SAR	150	150	150	150	260	1080

Source: EOS Reference Handbook, May 1993

APPENDIX B -- MICROGRAVITY EXPERIMENT CANDIDATE SUMMARY

(Sorted by payload weight less than 136 kg)

Payload Name	Mass (kg)	Mass (lb)	Power (Watts)		Dimension (cm)			Acceleration Level (g)	Run Time (hours)	Nonrecoverable Candidate
			Average	Peak	Length	Width	Height			
PPE	1	2	n/a	n/a	14	3.3	9	-	2	Y
ICE	2	3	n/a	n/a	9	9	18.4	-	1	Y
Candle Flames	4	8	2	12	12.1	12.1	19.1	-	0.5	Y
HPCG	4	9	n/a	n/a	35	2	13	-	-	-
FEA	12	26	-	-	47	37	19	-	-	Y
IBSE	25	55	125	125	47	40	18	-	continuous	-
IEF	29	64	7.3	30	53	48	23	-	1.5	-
SAMS (internal)	31	68	65	100	53	46	27	none	continuous	-
PCG	32	71	110	110	50	51	28	$1 \times 10(-2)$	-	-
ADSF	36	79	150	260	-	45 (dia)	49	-	-	-
GBX	45	100	257	257	-	-	-	-	24	Y
DCE	54	119	-	160	-	-	-	-	-	Y
CFTE	62	137	200	-	-	-	-	-	-	Y
SSCE	64	141	-	160	56	92	53	$1 \times 10(-3)$	0.7	Y
MLRS	71	157	75	382	27	35	41	-	20	-
PBE	75	165	210	300	-	15 (dia)	10	$1 \times 10(-3)$	3	Y
SAAL	82	181	2600	3100	-	40.5 (dia)	94	-	-	-
MSC	91	200	90	210	-	-	-	$1 \times 10(-2)$	4	Y
GAAS/GAS	91	201	200	280	-	50 (dia)	59	-	-	-
SAMS (external)	91	201	85	100	89	49	30	-	continuous	Y
VCGS	100	221	300	450	-	-	-	-	-	-
AADSF	120	265	920	920	-	43 (dia)	130	$1 \times 10(-4)$	continuous	-
IDGE	120	265	480	480	45	60	45	none	continuous	-
GFFC	133	293	262	-	-	-	-	-	-	-

Source: MSAMS Database and MSAD Information Summaries

105

REPORT DOCUMENTATION PAGE

Form Approved
OMB No. 0704-0188

1. AGENCY USE ONLY *(Leave blank)*	2. REPORT DATE	3. REPORT TYPE AND DATES COVERED
	July 1994	Contractor Report

4. TITLE AND SUBTITLE

Characterization of Spacecraft and Environmental Disturbances on a SmallSat

5. FUNDING NUMBERS

NAS1-18936
WU 233-01-01-01

6. AUTHOR(S)

Thomas A. Johnson, Dung Phu Chi Nguyen, Vince Cuda, and Doug Freesland

7. PERFORMING ORGANIZATION NAME(S) AND ADDRESS(ES)

CTA Incorporated
1 Enterprise Parkway Suite 390
Hampton, Virginia 23666

8. PERFORMING ORGANIZATION REPORT NUMBER

9. SPONSORING / MONITORING AGENCY NAME(S) AND ADDRESS(ES)

National Aeronautics and Space Administration
Langley Research Center
Hampton, Virginia 23681-0001

10. SPONSORING / MONITORING AGENCY REPORT NUMBER

NASA CR-194915

11. SUPPLEMENTARY NOTES

Langley Technical Monitor: William L. Grantham

12a. DISTRIBUTION / AVAILABILITY STATEMENT

Unclassified - Unlimited

Subject Category 18

12b. DISTRIBUTION CODE

13. ABSTRACT *(Maximum 200 words)*

The objective of this study is to model the on-orbit vibration environment encountered by a SmallSat. Vibration control issues are common to the Earth observing, imaging, and microgravity communities. A spacecraft may contain dozens of support systems and instruments, each a potential source of vibration. The quality of payload data depends on constraining vibration so that parasitic disturbances do not affect the payload's pointing or microgravity requirement. In practice, payloads are designed incorporating existing flight hardware in many cases with nonspecific vibration performance. Thus, for the development of a payload, designers require a thorough knowledge of existing mechanical devices and their associated disturbance levels. This study evaluates a SmallSat mission and seeks to answer basic questions concerning on-orbit vibration. Payloads were considered from the Earth observing, microgravity, and imaging communities. Candidate payload requirements were matched to spacecraft bus resources of present day SmallSats. From the set of candidate payloads, the representative payload GLAS (Geoscience Laser Altimeter System) was selected. The requirements of GLAS were considered very stringent for the 150 - 500 kg class of payloads. Once the payload was selected, a generic SmallSat was designed in order to accommodate the payload requirements (weight, size, power, etc.). This study seeks to characterize the on-orbit vibration environment of a SmallSat designed for this type of mission and to determine whether a SmallSat can provide the precision pointing and jitter control required for earth observing payloads.

14. SUBJECT TERMS

Smallsat, Pointing Jitter, Controls Structures Interaction

15. NUMBER OF PAGES

106

16. PRICE CODE

A06

17. SECURITY CLASSIFICATION OF REPORT	18. SECURITY CLASSIFICATION OF THIS PAGE	19. SECURITY CLASSIFICATION OF ABSTRACT	20. LIMITATION OF ABSTRACT
Unclassified	Unclassified		